

---

# PERIODIC ASYNCHRONY: An Effective Method for Accelerating On-Policy Reinforcement Learning

---

Jian Lu<sup>1</sup>

<sup>1</sup> Big Data&AI Lab, ICBC  
janelu@live.cn

## Abstract

Since the introduction of the GRPO algorithm, reinforcement learning (RL) has attracted increasing attention, with growing efforts to reproduce and apply it. However, training efficiency remains a critical challenge. In mainstream RL frameworks, inference and training are typically deployed on the same devices. While this approach reduces costs through resource consolidation, its synchronous execution imposes a computational coupling that prevents concurrent inference and training. In this study, we are returning to the strategy of separating inference and training deployment, and by introducing improvements in the data loader, we transform the conventional synchronous architecture into a periodically asynchronous framework, which allows for demand-driven, independent, and elastic scaling of each component, while the accuracy of the algorithm remains completely equivalent to the synchronization method, with both belonging to the on-policy strategy. It is worth emphasizing that we apply a unified tri-model architecture in the training phase, and we also proposed a shared-prompt attention mask to reduce repetitive computation. In practice, these works have achieved at least a threefold overall performance improvement in RL training on NPU platforms, indicating its potential for widespread application.

## 1 Introduction

In recent years, with the rapid development of large language models (LLMs), Reinforcement learning (RL) has once again become a key technique for post-training and human alignment. In particular, DeepSeek-R1 [5] introduced the Group Relative Policy Optimization (GRPO) algorithm, which successfully incentivized LLMs to exhibit stronger reasoning abilities in complex tasks. This work highlighted the potential of RL in improving reasoning and alignment in large models, and it has further stimulated widespread interest in efficient RL training methods across both academia and industry.

Nevertheless, despite the remarkable potential of RL in LLM alignment and reasoning tasks, training efficiency remains a critical challenge. This stems from the inherent complexity of the RL training pipeline. First, even the forward computation alone involves the primary training model (policy), an old policy model, and a reference model, while certain samples may additionally require a value model and a reward model [12], all of which substantially increase computational overhead. Second, before each training step, the latest weights of the policy model are often used to generate a large number of chain-of-thought (CoT) [16] trajectories to support optimization, further amplifying the inference burden. These factors not only constrain training throughput but also result in significant memory consumption, making efficiency improvements particularly challenging in large-scale model settings.

The optimization of reinforcement learning training has evolved continuously over time. Early DeepSpeed-Chat [17] primarily relied on ZeRO for distributed training, where the policy model itself was directly responsible for inference. This approach suffered from relatively low inference efficiency, which limited overall training throughput. Subsequently, an architecture that decouples inference from training is introduced, utilizing specialized inference engines such as vLLM [8] to generate responses. Although these approaches increased resource usage slightly, they significantly improved inference efficiency, thereby substantially enhancing overall training performance, as exemplified by Open-R1 [7]. To further leverage computing resources and reduce idle time between training and inference, the industry introduced training–inference co-location schemes. These approaches are conceptually still based on training–inference separation but deploy both tasks within the same resource pool, sharing resources through repeated task switching. Typical instances include OpenRLHF [6]. However, such architecture remain tightly coupled, limiting independent scalability and preventing training and inference from executing simultaneously. Beyond optimizing inference, additional exploration has focused on the training frameworks themselves. For example, MindSpeed-RL [3] and VERL [13] have adopted Megatron-style 3D parallelism [14] to train the policy model, improving throughput and enabling the training of larger models.

Against this backdrop, we revisit the inference–training separation strategy and enhance a conventional synchronous framework with new optimizations. Our approach builds on a Megatron-style 3D parallel architecture, further refined for improved training efficiency. Specifically, we add a background process in the data-loading module that acts as a producer, responsible for sending a full batch of prompts to the inference service. The main process acts as a consumer, immediately retrieving the outputs for training, where the received samples belonging to the same group are further divided into multiple micro-batches and trained sequentially. Once the entire batch has been consumed, the policy model’s weights are synchronized to the rollout workers, after which the next batch of asynchronous training begins. We refer to this mechanism as periodic asynchrony, which remains a purely on-policy asynchronous strategy and can thus be applied to any on-policy RL algorithm without modification. Benefiting from the decoupling of inference and training, the number of inference instances can be flexibly scaled according to inference efficiency, preventing inference from becoming the bottleneck. Furthermore, in GRPO, where each group of samples shares the same prompt, we propose a shared-prompt attention mask to reduce redundant computation and further improve efficiency. Experimental results demonstrate that, using 16 NPUs to train an 8B dense model with a 16k context length, our method achieves more than a threefold improvement in end-to-end RL training throughput.

## 2 Related Work

Improving the efficiency of reinforcement learning (RL) for large language models (LLMs) has been the subject of growing attention in both academia and industry. While synchronous frameworks dominate existing large-scale RL systems due to their algorithmic stability, they often suffer from underutilization of computational resources. To overcome these limitations, recent studies have explored asynchronous training paradigms, which aim to decouple inference from training and thereby enhance throughput and scalability. In this section, we review representative efforts in this direction, with a particular emphasis on asynchronous reinforcement learning approaches.

One of the earliest attempts in this direction is Asynchronous RLHF [11], which decouples the generation and learning processes, allowing new sample generation and old sample training to proceed in parallel. Its core idea is online but off-policy RLHF, where the model is updated using samples from previous iterations. While effective, this represents a typical off-policy strategy that may not directly apply to on-policy algorithms such as GRPO, and it remains constrained to relatively short-context settings.

Most recently, AReaL [4] advanced the application of asynchronous RL to LLM reasoning tasks. After we had already developed the methods presented in this paper, we became aware of AReaL, which fully decouples generation from training while introducing a parameter  $\eta$  to control data staleness. To better handle delayed samples, it incorporates a staleness-enhanced PPO variant, effectively modifying the on-policy paradigm to tolerate partially off-policy data. Additionally, its training start time depends on the completion of the first inference batch. Similarly, during the preparation of this manuscript, ROLL Flash [9] introduced a study sharing conceptual similarities with AReaL’s work. It also decouples training from inference and controls the proportion of off-policy data

through an async ratio. Both AReaL and ROLL Flash are off-policy asynchronous frameworks that improve training efficiency but require modifications to standard on-policy RL algorithms to handle data bias. This design trades a small portion of data originally intended for strictly on-policy training to avoid inference-service blocking, effectively shifting it toward off-policy learning. Although their experiments demonstrate the effectiveness of this biased setup, whether it generalizes across all RL algorithms and data regimes remains theoretically unproven.

However, they all fall under off-policy asynchronous frameworks, requiring control of data bias and modifications to algorithms to maintain stability for on-policy model training. Distinct from these approaches, our method introduces a new perspective with several key innovations:

1. **Periodic asynchrony**, which guarantees purely on-policy asynchronous acceleration without compromising algorithmic stability.
2. **Decoupling of prompt-level inference production and sample-level training consumption**, which maximally overlaps inference and training.
3. A **group-mask design** that enables effective reuse of forward and backward computations for prompt tokens, thereby reducing redundant computation.
4. A **distribution-consistent design** across the policy model, old-policy model, and reference model, allowing more flexible scaling and simplifying the overall system.
5. **Independent scalability** of inference and training instances, ensuring that neither component becomes a performance bottleneck.

Together, these designs enable efficient long-context training with substantially fewer computational resources. All the components have been implemented in the project release v5.0.5 on September 5, 2025 (<https://github.com/janelu9/EasyLLM>).

### 3 Background

#### Training RL with Micro-Batching

It is well known that when using distributed architectures for large-scale model pre-training or fine-tuning, one typically does not train on an entire batch and immediately update the model parameters with the resulting gradients, as is common in single-GPU training for small models. A full batch usually contains hundreds or even thousands of samples, and directly processing it in large-model training can easily lead to GPU out-of-memory (OOM) errors. Instead, the batch is divided into multiple micro-batches, each containing only one or two samples. These micro-batches are processed sequentially, with a buffer tensor used to accumulate the gradients from each micro-step. The accumulated gradients are applied to update the model parameters only after all micro-batches within the batch have been processed. In practice, these two training strategies are mathematically equivalent.

We can formally demonstrate the equivalence of full-batch and micro-batch training by reviewing the gradient update rules. When training on an entire batch directly, the model parameters are updated as follows:

$$W_{t+1} = W_t - \alpha \frac{1}{N} \sum_{n=1}^N g_n \quad (1)$$

where  $N$  is the total number of samples in the batch, and  $g_n$  denotes the gradient computed from the  $n$ -th sample.

For micro-batch training, the update proceeds differently. First, the accumulated gradient is initialized. Then, for each micro-batch  $j = 1$  to  $M$ , the gradient is updated as

$$g_{\text{acc}} := g_{\text{acc}} + \frac{1}{m} \sum_{i=1}^m g_{i,j}, \quad (2)$$

where  $m$  is the number of samples in each micro-batch, and  $g_{i,j}$  is the gradient of the  $j$ -th sample in the  $i$ -th micro-batch. Finally, after processing all micro-batches, the model parameters are updated

using the accumulated gradient:

$$W_{t+1} = W_t - \alpha \frac{1}{M} g_{\text{acc}}. \quad (3)$$

This formulation demonstrates that, mathematically, full-batch training and micro-batch training are equivalent. However, the micro-batch approach requires significantly less GPU memory. In particular, this delayed parameter update scheme is more suitable for reinforcement learning.

Consider the objective function of GRPO for generating responses from a single prompt:

$$J_{GRPO}(\theta) = \frac{1}{G} \sum_{i=1}^G \left( L_i(\pi_\theta \| \pi_{old}, A_i) - \beta D_{KL}^i(\pi_\theta \| \pi_{ref}) \right), \quad (4)$$

where

$$L_i(\pi_\theta \| \pi_{old}, A_i) = \min \left( \frac{\pi_\theta(o_i|q)}{\pi_{\theta_{old}}(o_i|q)} A_i, \text{clip} \left( \frac{\pi_\theta(o_i|q)}{\pi_{\theta_{old}}(o_i|q)}, 1 - \varepsilon, 1 + \varepsilon \right) A_i \right), \quad (5)$$

$$D_{KL}^i(\pi_\theta \| \pi_{ref}) = \frac{\pi_{ref}(o_i|q)}{\pi_\theta(o_i|q)} - \log \frac{\pi_{ref}(o_i|q)}{\pi_\theta(o_i|q)} - 1. \quad (6)$$

For a batch of  $N$  prompts, the objective function becomes:

$$\begin{aligned} J_{batch} &= \frac{1}{N} \sum_{i=1}^N J_{GRPO}^i \\ &= \frac{1}{N} \sum_{i=1}^N \frac{1}{G} \sum_{j=1}^G \left( L_{i,j} - \beta D_{KL}^{i,j} \right) \\ &= \frac{1}{NG} \sum_{i=1}^{NG} \left( L_i - \beta D_{KL}^i \right). \end{aligned} \quad (7)$$

Let

$$M = \frac{NG}{m}. \quad (8)$$

Then, the batch can be trained using micro-batches as:

$$J_{batch} = \frac{1}{M} \sum_{i=1}^M \frac{1}{m} \sum_{j=1}^m \left( L_{i,j} - \beta D_{KL}^{i,j} \right). \quad (9)$$

This demonstrates that reinforcement learning can also be trained using micro-batches. Compared with pre-training or fine-tuning, a batch now contains  $NG$  samples, but GPU memory usage is greatly reduced. Consequently, reinforcement learning can handle sequences as long as those supported during fine-tuning.

## 4 System Design

### 4.1 Unified Tri-Model Architecture

When performing reinforcement learning with large-scale models using different frameworks for inference and training—for instance, vLLM for inference and Megatron for training—the process generally involves three main steps:

1. Synchronize the weights of the policy model to the inference engine.
2. The inference engine retrieves prompts from the dataloader and generates responses. A reward module evaluates the generated responses based on the prompts, distinguishing high-quality responses from lower-quality ones.

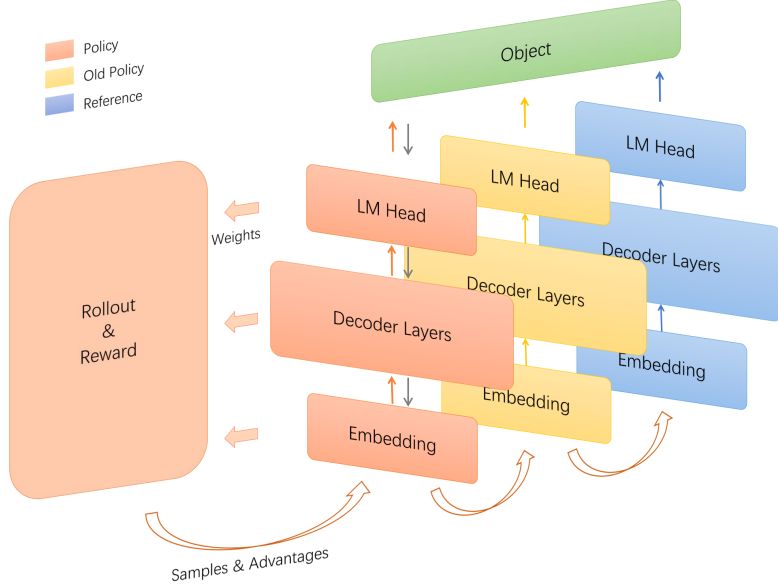


Figure 1: Architecture of unified triple models with shared distribution.

3. All generated samples and their associated scores are sent to the training engine for loss computation and backpropagation, updating the weights of the policy model.

For the third step, mainstream reinforcement learning systems typically require the computation of three types of logits in the forward pass: policy, old policy, and reference. These models share the same architecture, differing only in their weights. In this work, the training phase is implemented using a Megatron-like architecture, where a complete policy model is distributed across multiple computational units according to tensor parallelism and pipeline parallelism scales. During the forward computation of the old policy and reference models, each sub-network managed by the policy model is replicated twice across all computational units—once for computing the old policy logits and once for computing the reference logits. The reference network retains the original model weights, while the old policy network holds weights delayed by one training step relative to the policy model. The overall architecture of the reinforcement learning system constructed in this work is illustrated in Figure 1.

#### 4.2 Shared-Prompt Attention

In reinforcement learning training, each group of samples shares the same prompt. In fact, during micro-batch training, if the micro-batch size is greater than 1, the prompt can be reused. When the prompt contains many tokens while the generated responses are relatively short, reusing the prompt can significantly reduce redundant computation and GPU memory usage, thereby improving overall training efficiency.

Compared with standard training, when adopting the shared-prompt approach, the following adjustments are required:

1. Concatenate the shared prompt with the token IDs of multiple responses. Correspondingly, the labels used for computing probabilities should also be concatenated, except that the prompt portion does not need to be included in the labels.

$$\begin{cases} x = [x_p, x_{r_1}, x_{r_2}] \\ y = [y_{r_1}, y_{r_2}] \end{cases} \quad (10)$$

2. The position IDs need to be rearranged. For the second and subsequent responses, their starting positions should immediately follow the prompt, maintaining continuity with the prompt tokens.

$$p = (0, 1, \dots, |x_p| - 1, |x_p|, \dots, |x_p| + |x_{r_1}| - 1, |x_p|, \dots, |x_p| + |x_{r_2}| - 1) \quad (11)$$

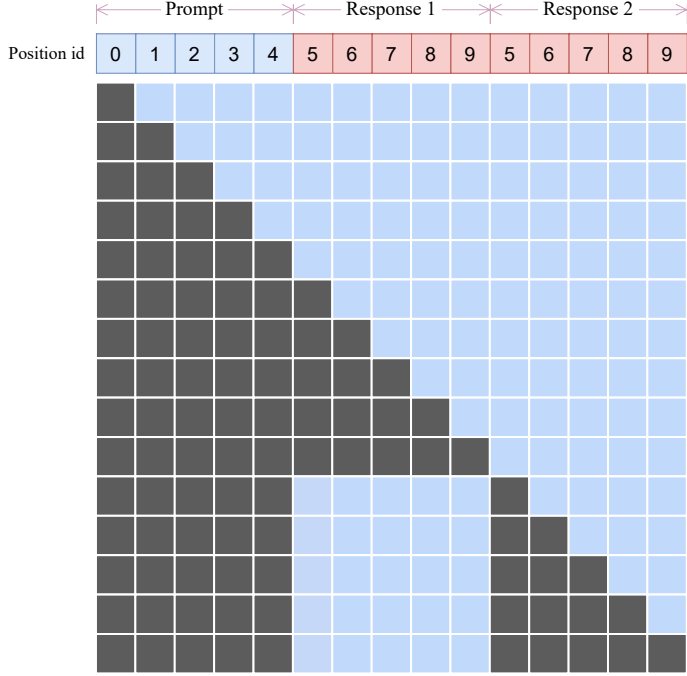


Figure 2: Shared-prompt attention mask.

3. In the attention module, use a group mask as illustrated in the Figure2, instead of the standard causal mask. This ensures that the value vectors of the second and subsequent responses are only aggregated with the prompt’s value vectors, and not with the value vectors of the preceding responses.

$$\begin{cases} \hat{y} = \text{model}(x, \text{mask}_{group}) \\ \hat{y}^{old} = \text{model}^{old}(x, \text{mask}_{group}) \\ \hat{y}^{ref} = \text{model}^{ref}(x, \text{mask}_{group}) \end{cases} \quad (12)$$

4. When computing probabilities, truncate the prompt tokens and retain only the response portion. Finally, the probabilities output by the three types of models, together with the reward scores, are fed into the GRPO objective function to compute the loss and perform iterative training.

$$\begin{cases} \pi = -\text{CrossEntropy}(\hat{y}_{|x_p|:|x|}, y) \\ \pi_{old} = -\text{CrossEntropy}(\hat{y}^{old}_{|x_p|:|x|}, y) \\ \pi_{ref} = -\text{CrossEntropy}(\hat{y}^{ref}_{|x_p|:|x|}, y) \\ Loss = J_{GRPO}(\pi, \pi_{old}, \pi_{ref}, A) \end{cases} \quad (13)$$

All other aspects remain the same as in standard training. This grouped micro-batch approach is generally more computationally efficient than simply concatenating micro-batches along the first axis, because the prompt tokens only need to be computed once, and padding is not required for shorter samples within a micro-batch. The advantage becomes especially pronounced when the prompt is long and the responses are relatively short.

### 4.3 Asynchronous On-Policy Reinforcement Learning

Asynchronous execution of inference and training is a key factor in accelerating reinforcement learning systems with a separated training-inference architecture. In such asynchronous systems, the critical aspect is minimizing the time the training engine waits for the rollout workers to return generated samples, i.e., the startup latency. In this work, we propose a simple approach that introduces a temporary data generator between the data loader and the trainer. This design transforms on-policy

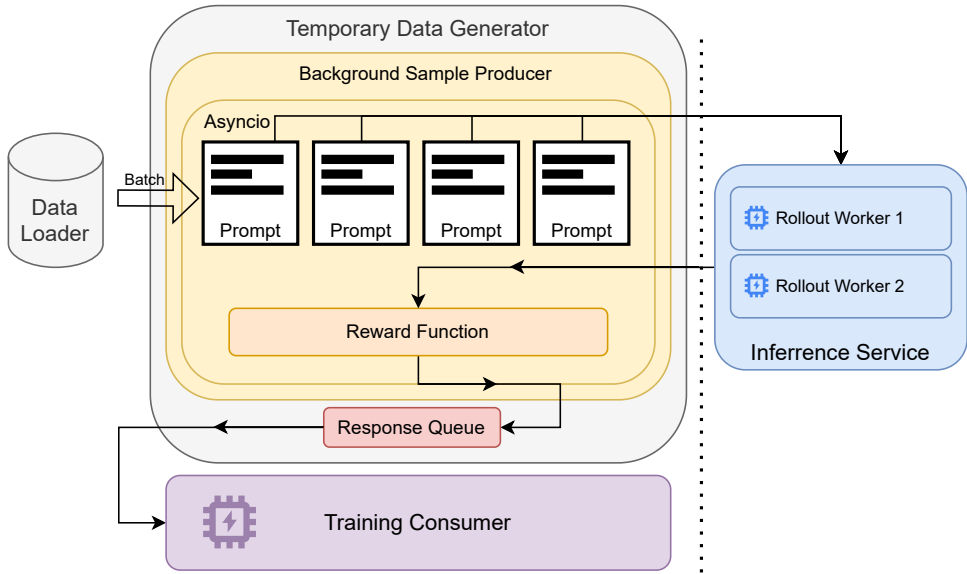


Figure 3: How our asynchronous system operates.

reinforcement learning from synchronous to asynchronous execution, significantly improving training efficiency without requiring any modifications to the underlying reinforcement learning algorithm. The reinforcement learning workflow incorporating the temporary sample generator is illustrated in Figure 3. It follows a typical *producer-consumer* pattern and consists of four main components:

1. **Data source**, which is the original data loader.
2. **Temporary data generator**, the additional component introduced in this work, which includes a background thread acting as a producer and a queue shared with the main process.
3. **Inference service**, responsible for receiving prompts and generating responses.
4. **Trainer**, which consumes the samples from the queue for training.

The core of our asynchronous design lies in the operation of the temporary generator. Within the temporary generator, a batch of prompts required for one training step is first retrieved from the standard data loader. A background thread is then launched to act as a *producer*. Inside this thread, a coroutine is used to concurrently and evenly dispatch the entire batch of prompts to multiple inference instances within the inference service. Upon receiving a large number of requests, the inference instances efficiently generate responses through continuous batching and return the completed responses back to the coroutine.

To fully exploit coroutine-level parallelism, the reward function is integrated directly into the coroutine. Each response returned by an inference instance is immediately scored, and once both inference and evaluation for a coroutine's assignment are finished, the resulting responses and reward scores are placed into a queue shared with the main process. This queue serves as a buffer that temporarily stores the generated responses from inference service.

The main process, acting as the *consumer*, continuously retrieves completed samples from the queue and feeds them to the three models for training. Under this design, the start time of training is determined by the earliest completed sample among all prompts in the batch. Once all prompts in the batch have been processed, the inference service enters an idle state until the training step finishes and the updated policy weights are synchronized back to the rollout workers. Only then does the next training cycle begin. Therefore, we refer to this design as **periodic asynchrony**.

In this way, the system constitutes a fully on-policy asynchronous reinforcement learning framework that remains decoupled from the underlying RL algorithm, meaning that no algorithmic modifications

---

**Algorithm 1** Periodic Asynchronous On-Policy Reinforcement Learning Algorithm

---

**Require:** Dataloader  $D$ , training iterations  $T$ , batch size  $B$   
**Ensure:** Trained policy model

- 1: Initialize shared queue  $Q$  and gradient accumulator  $O$
- 2: **for**  $t = 1$  to  $T$  **do**
- 3:     Synchronize policy model weights to the rollout workers
- 4:     Retrieve prompts  $P = \{p_1, \dots, p_B\}$  from  $D$
- 5:     Launch thread Producer:
- 6:         Create  $B$  concurrent coroutine tasks
- 7:         **Run in parallel for each**  $i = 1, \dots, B$ :
- 8:              $r_i \leftarrow \text{InferenceService}(p_i)$
- 9:              $a_i \leftarrow \text{RewardFunction}(r_i)$
- 10:             Enqueue  $(a_i, r_i)$  into  $Q$
- 11:      $O \leftarrow 0$
- 12:      $consumed\_count \leftarrow 0$
- 13:     **while**  $consumed\_count < B$  **do**
- 14:          $(a_i, r_i) \leftarrow \text{Dequeue}(Q)$
- 15:          $s_i \leftarrow \text{ProcessSample}(p_i, r_i)$
- 16:         Compute loss  $L(s_i)$  then backward
- 17:          $O \leftarrow O + \nabla L(s_i)$
- 18:          $consumed\_count \leftarrow consumed\_count + 1$
- 19:     **end while**
- 20:     Move policy's weights into old-policy's `state_dict`
- 21:     Update policy's weights using gradient  $O$
- 22: **end for**

---

are required to ensure correct operation within this asynchronous setup. Algorithm 1 is the pseudocode for the asynchronous reinforcement learning system proposed in this paper.

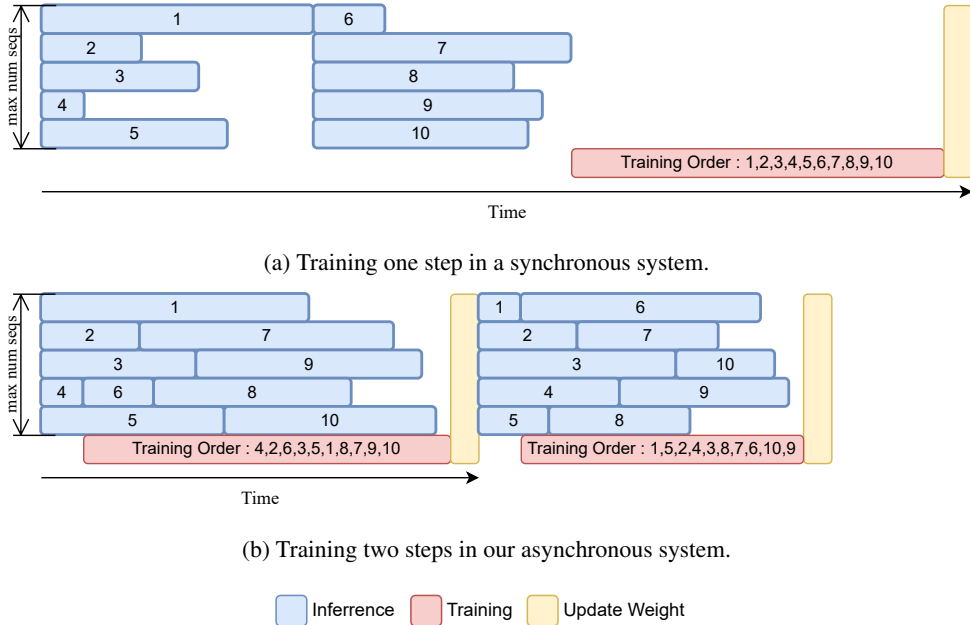


Figure 4: Comparison of training steps in synchronous and asynchronous systems.

Figure 4a and Figure 4b illustrate the differences between the asynchronous training system studied in this paper and a synchronous training system. It is evident that in a synchronous system, the training process must wait for all prompts to be processed by the inference service. If the batch size is large,

multiple inference batches may be required to complete all the prompts. The startup time for training is determined by the inference batches and the sum of the inference times of the slowest samples in each batch. Assuming the inference engine has a batch size of  $m$  and the prompts of one training batch are divided into  $n$  inference batches, the training startup time can be expressed as:

$$T_{sync} = \sum_{j=0}^n \max \left\{ t_i^j \mid i \in \{0, 1, \dots, m\} \right\} \quad (14)$$

Where  $t_i^j$  denotes the time required for the  $i$ -th prompt in the  $j$ -th batch to complete inference. In contrast, for an asynchronous system, the training startup time depends only on the earliest-completed prompt in the first inference batch, which can be expressed as:

$$T_{async} = \min \left\{ t_i^0 \mid i \in \{0, 1, \dots, m\} \right\} \quad (15)$$

Then, all samples in this batch are trained sequentially based on the order in which they enter the queue. Therefore, theoretically, if the training prompts in a batch cannot be processed by a single inference batch, the asynchronous system can achieve more than twice the speed of the synchronous system.

## 5 Implementation

The implementation in this study is based on the **PyTorch** training framework, with the training component using a 3D-parallel distributed architecture. Parts of the code from **Megatron-Core v0.8.0** are incorporated. On the **NPU platform**, additional components from **MindSpeed v2.1.0\_core\_r0.8.0**, **torch\_npu**, and several optimized operators included in **torch\_npu**—such as **npu\_fusion\_attention**, an accelerated attention kernel supporting custom masks, which is designed as a counterpart to **flash attention** [1]—are also employed.

For the inference component, **vLLM** is used as the engine, and on the NPU platform, **ascend\_vLLM 0.9.2.rc1** is adopted.

As in fine-tuning, all samples in the reinforcement learning training process are computed with their native sequence lengths for both forward and backward passes, without any additional padding; that is, the system uses **dynamic-length training**.

## 6 Experiments

This study primarily conducts comparative experiments on mathematical reasoning tasks. The reinforcement learning frameworks included in the comparison are: MindSpeed-RL, which adopts a training–inference shared-resource architecture; the synchronous reinforcement learning version implemented in this work under a training–inference decoupled design; and the asynchronous reinforcement learning version proposed in this study.

The main objective is to experimentally validate the performance between periodic asynchronous and synchronous training, as well as to compare the proposed periodic asynchronous system with other mainstream synchronous reinforcement learning frameworks on the same platform, while also evaluating the scalability of our periodic asynchronous system.

The primary evaluation metric is the end-to-end training throughput, such as the average number of tokens trained per second per device (TPSPD). This is calculated as the total number of tokens processed over several steps divided by the total elapsed time and then divided by the number of devices used.

Since no modifications were made to the reinforcement learning algorithm, accuracy metrics are reported only for reference, primarily to verify the correctness of algorithm reproduction.

### 6.1 Model and Environment Configuration

The models compared in this section are Qwen3-8B [15] and DeepSeek-R1-Distill-Qwen-32B [2] (since the current version of Mindspeed-RL does not yet support reinforcement learning training for Qwen3-32B, we instead use DeepSeek-R1-Distill-Qwen-32B as the training model.). The training

data comes from the publicly available math problem dataset DeepScaler [10]. All reinforcement learning experiments use the GRPO algorithm. The accuracy test set is the AIME24 [18].

## 6.2 Comparison between Asynchronous and Synchronous Training

In the first set of experiments, Qwen3-8B was used as the training model, with a context length of 16k. A total of 16 NPUs were used. For the synchronous and asynchronous training configurations implemented in this work under the training–inference decoupled architecture, 8 NPUs were allocated to launch a single training instance with tensor parallelism (TP = 8) and pipeline parallelism (PP = 1). The remaining 8 NPUs were used to launch four inference instances with TP = 2. For MindSpeed-RL, the training configuration used 16 NPUs to launch two training instances (TP = 8, PP = 1), while all 16 NPUs were also used to launch eight inference instances (TP = 2).

Table 1: Accuracy and training efficiency comparison results on Qwen3-8B. Each framework was trained for 100 steps, and the total time consumed and the total number of tokens trained were extracted from the logs.

Framework	GRPO Steps	AIME24	Trained Tokens	Training Hours	NPUs	Tokens/sec/device
Baseline	0	0.725	0	0	0	-
MindSpeed-RL	100	0.733	706.355M	198.942	16	61.641
Sync (our)	100	0.746	827.306M	143.678	16	99.966
Async (our)	100	0.758	917.609M	82.861	16	192.259

In terms of TPSPD, the training speed ratio among the three implementations was 1:1.62:3.12. For accuracy evaluation, we adopted a rule-based method, where the final answer predicted by the policy model is considered correct if it can be correctly extracted and matches the ground-truth answer in the dataset; otherwise, it is considered incorrect. The tests were conducted using the inference engine vLLM 0.9.1.rc, with an output length limit of 32k. Each test sample was evaluated 8 times, with inference parameters set to temperature = 0.7, top\_p = 0.95, and top\_k = 20. In total, 240 test problems were evaluated. It is evident that the models trained by the three frameworks achieved similar accuracy on the AIME24 benchmark, with variations within normal random fluctuations, supporting the equivalence in effectiveness between the asynchronous and synchronous methods implemented in this work.

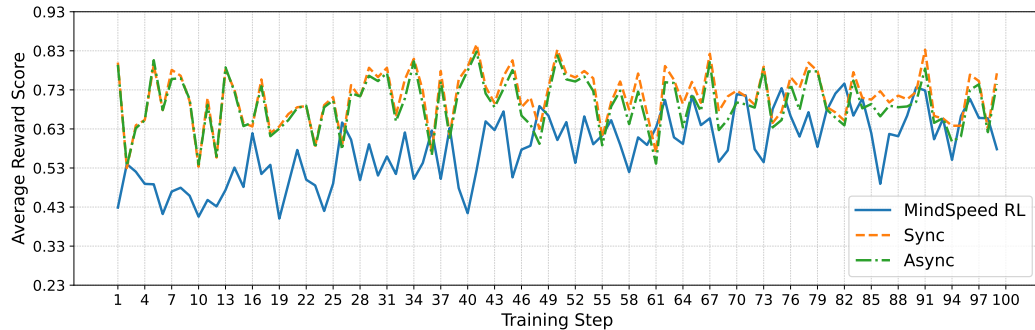


Figure 5: Training step-wise average reward score comparison

We also monitored the reward scores throughout the training process of the three frameworks, as depicted in Figure 5. The reward score trajectories of our synchronous and asynchronous methods are nearly indistinguishable, further reinforcing the assertion that the proposed asynchronous approach is computationally equivalent to its synchronous counterpart. Both curves show a slight upward trend, which can likely be attributed to the baseline model having already been pre-trained on similar data. Notably, in the initial phases of training, the reward mean curve for Mindspeed-RL diverges significantly from that of our approach. This disparity may arise from differences in system architecture. Additionally, it is important to note that, in contrast to our environment, Mindspeed-RL utilizes vLLM version 0.9.1 and vllm\_ascend version 0.9.0rc2.

The model used in the second set of experiments is DeepSeek-R1-Distill-Qwen-32B, with a context length of 16k, and only two experiments are conducted. For our asynchronous framework, the configuration is as follows: 32 NPUs are used to launch a single training instance with TP = 8 and

$PP = 4$ , while the remaining 16 NPUs are used to launch four inference instances with  $TP = 4$ . In contrast, for the Mindspeed-RL configuration, 64 NPUs are used to launch two training instances with  $TP = 8$  and  $PP = 4$ , and simultaneously, the same 64 NPUs are used to launch 16 inference instances with  $TP = 4$ .

Table 2: Accuracy and training efficiency comparison results on DeepSeek-R1-Distill-Qwen-32B. Each framework was trained for 20 steps, and the total time consumed and the total number of tokens trained were extracted from the logs.

Framework	GRPO Steps	AIME24	Trained Tokens	Training Hours	NPUs	Tokens/sec/device
Baseline	0	0.726	0	0	0	-
MindSpeed-RL	20	0.679	105.678M	69.116	64	6.636
Async (our)	20	0.737	123.999M	21.453	48	33.449

The evaluation methodology is identical to that used in the first set of experiments. According to the results, for the 32B-scale model, the ratio of the TPSPD metric between Mindspeed-RL and our asynchronous framework is 1 : 5.05.

Combining the results of the two experimental groups, we obtain a clear comparative plot of the training speeds, as shown in Figure 6.

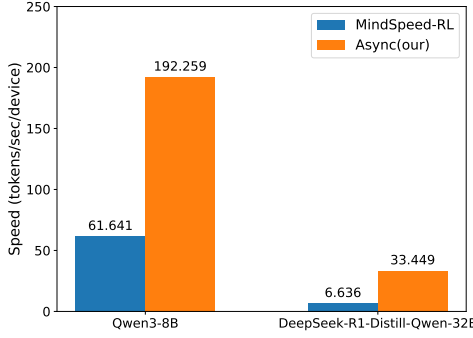


Figure 6: TPSPD between MindSpeed-RL and Async(ours)

### 6.3 Asynchronous Scalability Experiments

We also conducted a set of experiments to evaluate the scalability of our framework, using the same configuration as in the first experiment group. Under an inter-node bandwidth of 100 Gb/s, the results are shown in Table 3.

Table 3: Scalability comparison results. TPSPD performance of training Qwen3-8B on 16, 32, and 64 NPUs using our asynchronous framework.

Model	NPUs	Training Instance	Inference Instance	Training Steps	Tokens/sec/device
Qwen3-8B	16	1	4	20	188.162
	32	2	8	20	171.824
	64	4	16	20	163.208

When expressed in TPS (tokens per second), the results are more intuitively illustrated in Figure 7. Training with 32 NPUs shows a  $1.83\times$  speedup compared to 16 NPUs, while using 64 NPUs results in a  $1.9\times$  speedup over 32 NPUs. Overall, the proposed asynchronous reinforcement learning framework demonstrates near-linear scaling in training speed as the number of devices increases.

## 7 Conclusion

This paper presents an asynchronous on-policy reinforcement learning implementation that maintains the same training stability as synchronous RL methods. The feasibility of performing reinforcement

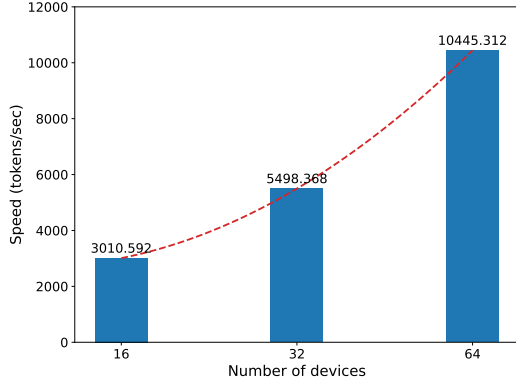


Figure 7: TPS of our framework under different scales of data parallelism

learning training with micro-batches is theoretically demonstrated. Prompt-level asynchronous parallelism maximizes the overlap between inference and training. During training, a three-mode (policy, old policy, reference) unified and identically distributed architecture is introduced, along with a group-mask attention mechanism that provides clear advantages when prompts are long and responses are short.

Experiments show that the proposed framework achieves a three- to five-fold improvement in end-to-end performance over current mainstream RL training frameworks on the NPU platform. The results also support the equivalence in training effectiveness between the asynchronous and synchronous methods. Furthermore, the decoupling of training and inference allows both to be scaled independently and flexibly, achieving optimal balance and maximizing the speed-to-device ratio. The decoupling of training architecture and algorithm also implies that the proposed framework can be applied to other on-policy reinforcement learning algorithms without any modifications for compatibility with asynchronous training architectures.

## References

- [1] T. Dao. Flashattention-2: Faster attention with better parallelism and work partitioning. *arXiv preprint arXiv:2307.08691*, 2023.
- [2] DeepSeek-AI. Deepseek-r1: Incentivizing reasoning capability in llms via reinforcement learning, 2025. URL <https://arxiv.org/abs/2501.12948>.
- [3] L. Feng, C. Pan, X. Guo, F. Mei, B. Ning, J. Zhang, X. Liu, B. Zhou, Z. Shu, C. Liu, G. Yang, Z. Han, J. Wang, and B. Wang. Mindspeed rl: Distributed dataflow for scalable and efficient rl training on ascend npu cluster, 2025. URL <https://arxiv.org/abs/2507.19017>.
- [4] W. Fu, J. Gao, X. Shen, C. Zhu, Z. Mei, C. He, S. Xu, G. Wei, J. Mei, J. Wang, T. Yang, B. Yuan, and Y. Wu. Areal: A large-scale asynchronous reinforcement learning system for language reasoning, 2025. URL <https://arxiv.org/abs/2505.24298>.
- [5] D. Guo, D. Yang, H. Zhang, J. Song, P. Wang, Q. Zhu, R. Xu, R. Zhang, S. Ma, X. Bi, et al. Deepseek-r1 incentivizes reasoning in llms through reinforcement learning. *Nature*, 645(8081): 633–638, 2025.
- [6] J. Hu, X. Wu, Z. Zhu, Xianyu, W. Wang, D. Zhang, and Y. Cao. Openrlhf: An easy-to-use, scalable and high-performance rlhf framework. *arXiv preprint arXiv:2405.11143*, 2024.
- [7] Hugging Face. Open r1: A fully open reproduction of deepseek-r1, January 2025. URL <https://github.com/huggingface/open-r1>.
- [8] W. Kwon, Z. Li, S. Zhuang, Y. Sheng, L. Zheng, C. H. Yu, J. E. Gonzalez, H. Zhang, and I. Stoica. Efficient memory management for large language model serving with pagedattention. In *Proceedings of the ACM SIGOPS 29th Symposium on Operating Systems Principles*, 2023.
- [9] H. Lu, Z. Liu, S. Xiong, Y. He, W. Gao, Y. Wu, W. Wang, J. Liu, Y. Li, H. Zhao, J. Huang, S. Yang, X. Li, Y. Luo, Z. Liu, L. Pan, J. Yan, W. Wang, W. Su, J. Wang, L. Qu, and B. Zheng.

Part ii: Roll flash – accelerating rlvr and agentic training with asynchrony, 2025. URL <https://arxiv.org/abs/2510.11345>.

- [10] M. Luo, S. Tan, J. Wong, X. Shi, W. Tang, M. Roongta, C. Cai, J. Luo, T. Zhang, E. Li, R. A. Popa, and I. Stoica. Deepscaler: Surpassing 01-preview with a 1.5b model by scaling rl. <https://pretty-radio-b75.notion.site/DeepScaleR-Surpassing-01-Preview-with-a-1-5B-Model-by-Scaling-RL-19681902c1468005bed8ca303013a4e2>, 2025. Notion Blog.
- [11] M. Noukhovitch, S. Huang, S. Xhonneux, A. Hosseini, R. Agarwal, and A. Courville. Asynchronous rlhf: Faster and more efficient off-policy rl for language models. *arXiv preprint arXiv:2410.18252*, 2024.
- [12] J. Schulman, F. Wolski, P. Dhariwal, A. Radford, and O. Klimov. Proximal policy optimization algorithms. *arXiv preprint arXiv:1707.06347*, 2017.
- [13] G. Sheng, C. Zhang, Z. Ye, X. Wu, W. Zhang, R. Zhang, Y. Peng, H. Lin, and C. Wu. Hybridflow: A flexible and efficient rlhf framework. *arXiv preprint arXiv: 2409.19256*, 2024.
- [14] M. Shoeybi, M. Patwary, R. Puri, P. LeGresley, J. Casper, and B. Catanzaro. Megatron-lm: Training multi-billion parameter language models using model parallelism. *arXiv preprint arXiv:1909.08053*, 2019.
- [15] Q. Team. Qwen3 technical report, 2025. URL <https://arxiv.org/abs/2505.09388>.
- [16] J. Wei, X. Wang, D. Schuurmans, M. Bosma, F. Xia, E. Chi, Q. V. Le, D. Zhou, et al. Chain-of-thought prompting elicits reasoning in large language models. *Advances in neural information processing systems*, 35:24824–24837, 2022.
- [17] Z. Yao, R. Y. Aminabadi, O. Ruwase, S. Rajbhandari, X. Wu, A. A. Awan, J. Rasley, M. Zhang, C. Li, C. Holmes, Z. Zhou, M. Wyatt, M. Smith, L. Kurilenko, H. Qin, M. Tanaka, S. Che, S. L. Song, and Y. He. DeepSpeed-Chat: Easy, Fast and Affordable RLHF Training of ChatGPT-like Models at All Scales. *arXiv preprint arXiv:2308.01320*, 2023.
- [18] Y. Zhang and T. Math-AI. American invitational mathematics examination (aime) 2024, 2024.